

Effect of H₂O₂ modification of H₃PW₁₂O₄₀@carbon for m-xylene oxidation to isophthalic acid

Zhou-wen Fang, Di Wen, Zhi-hao Wang, and Xiang-li Long[†]

State Key Laboratory of Chemical Engineering, East China University of Science and Technology,
Shanghai 200237, P. R. China

(Received 29 March 2018 • accepted 31 July 2018)

Abstract—The production of isophthalic acid (IPA) from the oxidation of m-xylene (MX) by air is catalyzed by H₃PW₁₂O₄₀ (HPW) loaded on carbon and cobalt. We used H₂O₂ solution to oxidize the carbon to improve the catalytic activity of HPW@C catalyst. Experiments reveal that the best carbon sample is obtained by calcining the carbon at 700 °C for 4 h after being impregnated in the 3.75% H₂O₂ solution at 40 °C for 7 h. The surface characterization displays that the H₂O₂ modification leads to an increase in the acidic groups and a reduction in the basic groups on the carbon surface. The catalytic capability of the HPW@C catalyst depends on its surface chemical characteristics and physical property. The acidic groups play a more important part than the physical property. The MX conversion after 180 min reaction acquired by the HPW@C catalysts prepared from the activated carbon modified in the best condition is 3.81% over that obtained by the HPW@C catalysts prepared from the original carbon. The IPA produced by the former is 46.2% over that produced by the latter.

Keywords: Isophthalic Acid, Activated Carbon, H₃PW₁₂O₄₀, H₂O₂, m-Xylene

INTRODUCTION

Isophthalic acid (IPA) is widely used in the production of unsaturated polyester resins, alkyd resins, polyaramides and other chemical products. It is generally manufactured through the oxidation of m-xylene (MX) by air under the catalysis of homogeneous Co/Mn/Br catalyst system in acetic acid [1]. However, the bromide in the catalyst system may seriously erode the equipment and pollute the environment. It is of great significance to develop a technology for the production of IPA by bromine-free catalytic system.

Heteropoly acid (HPA) is widely used in many homogeneous and heterogeneous catalytic reactions. Xu et al. [2] applied H₃PW₁₂O₄₀/γ-Fe₂O₃ for alkylation of thiophene with olefine. Lv et al. [3] reported a H₃PW₁₂O₄₀/Co(OAc)₂/Mn(OAc)₂ catalyst system to manufacture IPA in homogeneous reaction system and avoided the adverse effect of bromine. Long et al. [4] put forward a heterogeneous system composed of H₃PW₁₂O₄₀/carbon and Co(OAc)₂ to catalyze the oxidation of MX to IPA and got a higher MX oxidation rate and IPA yield than the H₃PW₁₂O₄₀/Co(OAc)₂/Mn(OAc)₂ catalyst system.

Activated carbon has a well-developed pore structure and abundant surface chemical groups. The change of the physical structure and surface chemistry concerns the improvement of adsorption capacity and catalytic activity of activated carbon [5-8]. Guo et al. [9] realized the selective catalytic reduction of NO with NH₃ over H₂SO₄ modified activated carbons. Park et al. [10] applied MnO/C nanocomposite for high performance lithium-ion battery anodes.

Liu et al. [11] enhanced the removal of methyl mercaptan with metal modified activated carbon. Wang et al. [12] modified the carbon with HNO₃ solution to improve the catalytic activity of H₃PW₁₂O₄₀@carbon catalyst in the oxidation of MX to IPA. The results obtained implied that the acidic functional groups on the carbon surface played a vital role in improving the catalytic ability of the H₃PW₁₂O₄₀@C catalyst.

H₂O₂ usually functions as an oxidant to introduce oxygen-containing acidic groups to the activated carbon surface. Chen et al. [13] found that the decolorization of caramel, methylene blue adsorption, phenol adsorption and iodine number of granular fir-based activated carbon could be improved with H₂O₂ modification. Xue et al. [14] enhanced the lead sorption ability of the biochar by modifying the char with H₂O₂. Song et al. [15] increased the amount of oxygen-containing groups and the homogeneous active sites available for the adsorption of Pb²⁺ on the activated carbon surface by oxidizing the carbon with H₂O₂. We used H₂O₂ solution to treat the coconut activated carbon to ameliorate the catalytic ability of HPW@C catalyst in the production of IPA from MX. The modification conditions were explored systematically. The change of the surface chemistry and the physical structure of activated carbon is characterized to study the relationship between the structure of the activated carbon and the catalytic activity of HPW@C catalyst.

EXPERIMENTAL SECTION

1. Materials

The coconut activated carbon used was produced by Shanghai Activated Carbon Co., Ltd., China. The cobalt acetate tetrahydrate and phosphotungstic acid were produced by Sinopharm Chemical Reagent Co., Ltd. IPA, MX, m-tolualdehyde (3-IMA), M-Toluic

[†]To whom correspondence should be addressed.

E-mail: longdragon@ecust.edu.cn

Copyright by The Korean Institute of Chemical Engineers.

acid (M-TA) and 3-carboxybenzaldehyde (3-CBA) were from Energy Chemicals Co., Ltd. Glacial acetic acid, H₂O₂ (30%), potassium dihydrogen phosphate and phosphoric acid were manufactured by Shanghai Lingfeng Chemical Reagent Co., Ltd. All these reagents are of analytically grade. Acetonitrile and methanol are of chromatographic grade and were supplied by J&K Scientific Ltd.

2. Modification of Activated Carbon

The activated carbon of 20-40 mesh was chosen as the HPW loader. After being washed with deionized water repeatedly, the carbon sample was dried at 110 °C until its weight was constant and then sealed for use.

In a typical modification process, 20 g activated carbon was impregnated in 100 mL H₂O₂ solution for several hours, followed by being rinsed with deionized water repeatedly and dried to constant weight at 110 °C. Then the sample was heated in a furnace at high temperature for some hours under N₂ atmosphere.

3. Preparation of H₃PW₁₂O₄₀@C Catalyst

15 g activated carbon sample was soaked in 60 mL phosphotungstic acid (HPW) solution of 18.75 g L⁻¹ at 60 °C for 4 h. Then the mixture was heated at 100 °C to vaporize the water. The carbon sample loaded with HPW was vacuum dried at 110 °C for 12 h. The H₃PW₁₂O₄₀@C catalyst was prepared after the carbon immobilized with H₃PW₁₂O₄₀ being calcined in N₂ at 220 °C for 4 h.

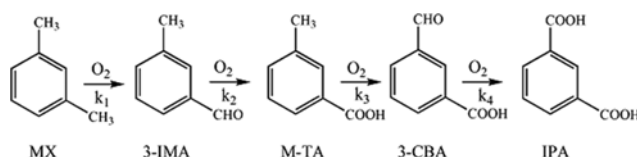


Fig. 1. Simplified reaction path for the oxidation of m-xylene to isophthalic acid.

4. Analytical Methods

In terms of the simplified reaction path from MX to IPA in Fig. 1, MX, 3-IMA, M-TA, 3-CBA and IPA coexist in the liquor. The liquid samples were tested by HPLC equipped with a C18 chromatographic column.

Table 1. Standard equations

Sample	Standard equations	R ²
IPA	$Y_{IPA} = 1.58796 \times 10^{-10} X_{IPA} + 1.26058 \times 10^{-6}$	0.99931
3-CBA	$Y_{3-CBA} = 1.74589 \times 10^{-10} X_{3-CBA} - 1.28407 \times 10^{-6}$	0.99936
m-TA	$Y_{m-TA} = 1.27313 \times 10^{-10} X_{m-TA} - 6.25067 \times 10^{-7}$	0.99966
3-MB	$Y_{3-MB} = 4.49980 \times 10^{-10} X_{3-MB} - 3.49858 \times 10^{-6}$	0.99986
MX	$Y_{MX} = 3.43066 \times 10^{-10} X_{MX} - 3.52656 \times 10^{-6}$	0.99937

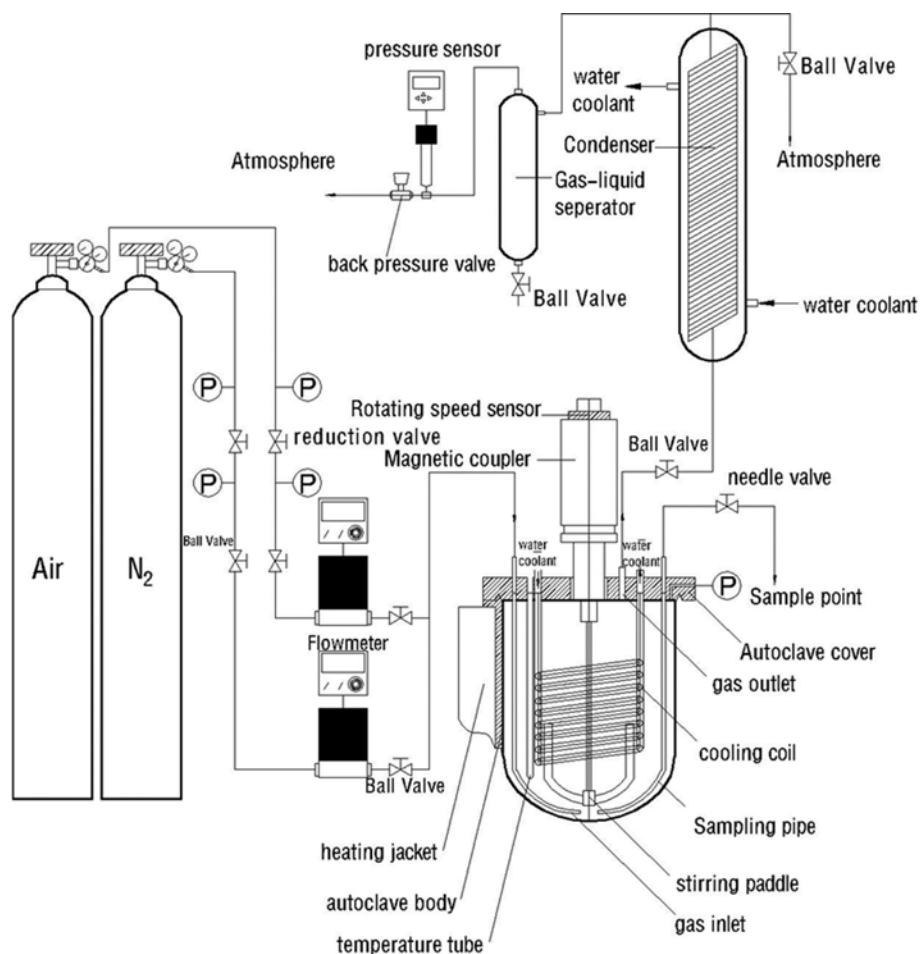


Fig. 2. Schematic of the experimental setup.

graphic column and a UV-detector. The mobile phase of HPLC was composed of 80% acetonitrile solution and 0.03 mol l^{-1} KH_2PO_4 aqueous solution. The CH_3CN/KH_2PO_4 ratio of the mobile phase altered from 1:4 (volume) to 4:1 after the mobile phase ran for 30 min at 1.0 ml min^{-1} . IPA, 3-IMA, m-TA and 3-CBA were measured by UV-detector at 230 nm, while MX was detected at 220 nm. The concentrations of these constituents were calculated by external standard method. The standard equations obtained with standard solutions are in Table 1, where X_i means peak area and Y_i stands for the mass concentration with unit of $g\ g^{-1}$.

5. Experimental Setup and Procedure

The experiments for the catalytic oxidation of MX to IPA were performed in the setup shown in Fig. 2. The oxidation reactor was a titanium autoclave of 1,000 ml. The complete condensation and recycling of the evaporated compounds was ensured with a condenser, a gas-liquid separator and a liquid recycle tank. The reaction heat was removed immediately by a cooling coil fixed in the autoclave. The reaction temperature was adjusted by the electric heating jacket with a precision of 0.2 °C. The pulsation of the pressure in the autoclave was below 2 KPa. The amount of HPW@C supported with 7.5% (wt) $H_3PW_{12}O_{40}$ (HPW) on the carbon in the reaction liquor was 16.0 g l^{-1} . The Co(II) concentration in the reaction liquor was 0.069% (wt). The initial MX concentration is 3.53% (wt).

The pressure in the autoclave was raised to 3.0 MPa with N_2 after the autoclave was filled with a mixture of proposed amount of HAc, H_2O , MX, $Co(OAc)_2$ and HPW@C. Then the stirring speed of the magnetic stirrer was controlled at 300 rpm before beginning heating the autoclave. The catalytic oxidation of MX to IPA was started when air was introduced into the autoclave with a rate of 1.0 L min^{-1} as soon as the temperature in the autoclave reached 200 °C. Liquor was sampled from the autoclave every 30 min to determine the MX conversion and the concentration of the products.

6. Characterization of the Carbon Sample

Quantachrome NOVA4200e Specific Surface and Porosity Analyzer was used to obtain the textural characterization of the samples by conducting N_2 adsorption/desorption at $-195.7\ ^\circ C$ after the samples had been heated for 8 h at 200 °C. Total surface area was obtained with BET model. Total pore volume was converted from N_2 adsorption volume at $P/P_0=0.9876$. The micropore specific surface and micropore volume was computed with t-plot method, and the average pore size was calculated in terms of BJH analyses.

Acid-base titration method proposed by Boehm [16] was used to measure the amount of the surface functional groups and characterize the amphoteric characteristics of the modified activated carbon.

X-ray photoelectron spectroscopy (XPS) measurements were performed by Thermo Scientific EscaLab 250Xi X-ray photoelectron spectrometer at monochromated Al-Ka anode X-ray radiation (1,486.6 eV). FT-IR spectra were obtained with Nicolet 6700 Fourier transform spectrophotometer using pellets of KBr disks containing carbon samples at resolution of 4 cm^{-1} in the range of 400-4,000 cm^{-1} .

RESULTS AND DISCUSSION

1. Effect of H_2O_2 Concentration

The oxidation rate of the carbon by H_2O_2 is determined by H_2O_2

concentration. It is necessary to test the impact of H_2O_2 concentration on the catalytic performance of $H_3PW_{12}O_{40}@C$ catalyst. Five carbon samples were soaked in H_2O_2 solution of 1.50%, 3.00%, 3.75%, 4.50%, and 5.25%, respectively, at 45 °C for 8 h. Then the samples obtained were calcined at 700 °C for 4 h. The $H_3PW_{12}O_{40}@C$ catalyst prepared with the modified carbon samples and the original carbon were used to accelerate the oxidation of MX to IPA. The catalytic capacities of these $H_3PW_{12}O_{40}@C$ catalysts can be compared in terms of the experimental results shown in Fig. 3.

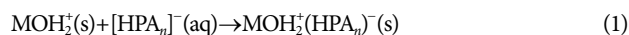
It can be seen from Fig. 3(a) that H_2O_2 modification improves the catalytic activity of the $H_3PW_{12}O_{40}@C$ catalyst. The $H_3PW_{12}O_{40}@C$ catalyst prepared with the modified carbon accelerates the MX oxidation more efficiently. After 180 min, the MX conversion obtained by the catalyst prepared from the carbon modified with 3.75% H_2O_2 was 97.57% while that by the $H_3PW_{12}O_{40}@C$ catalyst prepared with the original carbon was 95.39%. The MX conversions obtained by the catalyst prepared from the carbon modified with H_2O_2 solution of 1.50%, 3.00%, 4.50% and 5.25% were 97.34%, 97.35%, 96.24% and 96.84%, respectively. It can also be concluded that it will not upgrade the MX conversion further if the H_2O_2 concentration is raised above 3.75%.

Fig. 3(c) suggests that the formation rate of m-TA catalyzed by the catalyst prepared from modified activated carbon be quicker than that of the catalyst prepared from original carbon within the 120 min operation. 120 min later, the depletion rate of m-TA got by the $H_3PW_{12}O_{40}@C$ catalyst prepared with the modified activated carbon exceeded the generation rate of m-TA and the m-TA concentration began to decrease. But the m-TA by the HPW@C catalyst prepared with the original carbon kept going up. It can be concluded that the 3-IMA oxidation rate and the m-TA oxidation rate acquired by the modified samples are greater than those obtained by the original one.

Fig. 3(e) demonstrates that the modified samples are able to produce more IPA than the original one. The sample treated with 3.75% H_2O_2 solution acquires more IPA than any other samples. After 180 min operation, the IPA obtained by the $H_3PW_{12}O_{40}@C$ catalyst prepared from the sample modified with 3.00%, 3.75% and 4.50% H_2O_2 reaches 1.84% (wt), 2.05% (wt) and 1.89% (wt), while that by the $H_3PW_{12}O_{40}@C$ catalyst prepared from the original carbon was only 1.43% (wt). The experiments prove that the best H_2O_2 concentration is 3.75%.

To explain the amelioration of the catalytic ability of the $H_3PW_{12}O_{40}@C$ catalyst resulting from the modification with H_2O_2 solution, surface characterization was done to illustrate the relationship between the surface characteristics of the carbon samples and the catalytic activity of the $H_3PW_{12}O_{40}@C$ catalysts.

The chemical groups on the carbon surface affect the adsorption capacity and catalytic activity of activated carbon, among which the most important groups are oxygen-containing groups and nitrogen-containing groups [17]. The surface chemistry of activated carbon has a significant impact on the load of HPW [18,19]. Hydroxyl hydrogenated on the carbon surface and heteropoly acid anion forms a complex in acidic environment as follows:



Small amount of transition metal(M) exists on the carbon sur-

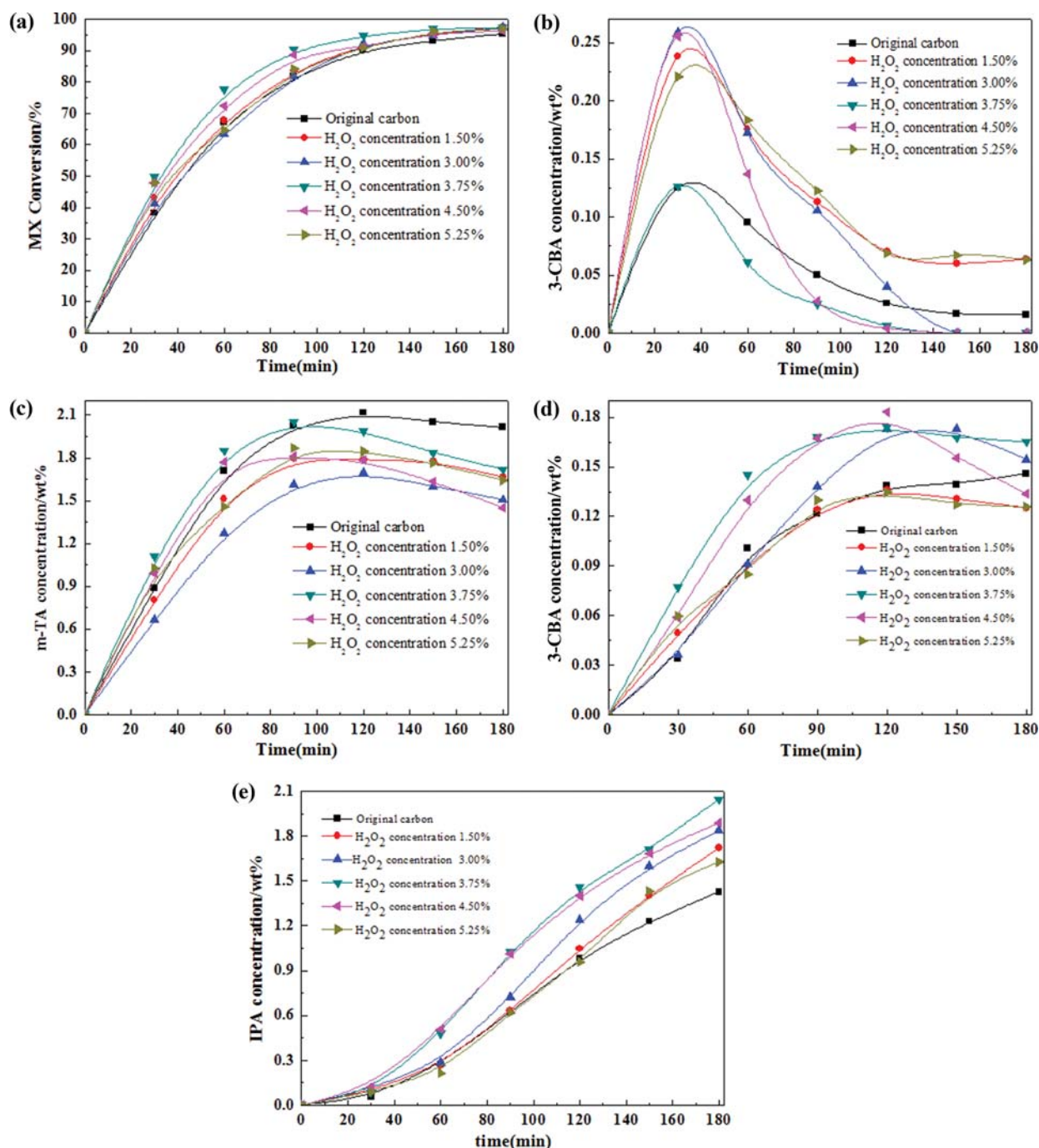


Fig. 3. Effect of H₂O₂ concentration on MX oxidation. 215 °C, 3.0 MPa, air fluent: 1.0 L min⁻¹, stirring speed: 300 r/min, HPW@C: 16 g l⁻¹, MX: 3.53% (wt), Co²⁺: 0.069% (wt), H₂O: 4.0% (wt), HAC: 400 ml.

face and transition metal, which catalyzes the decomposition of H₂O₂ to hydroxyl radicals (HO·) in solution as follows:



H₂O₂ will decompose to HOO⁻ under alkaline condition as follows:



HOO· is a free radicals with strong electrophilic ability and oxidizability, which can combine with carbon to form phenolic hydroxyl [20] or take off hydrogen atoms of C-H to generate C=O. Meanwhile, some groups can be oxidized by HOO· to quinone, benzopyran or pyrene [21]. HOO⁻ is a nucleophile that can react

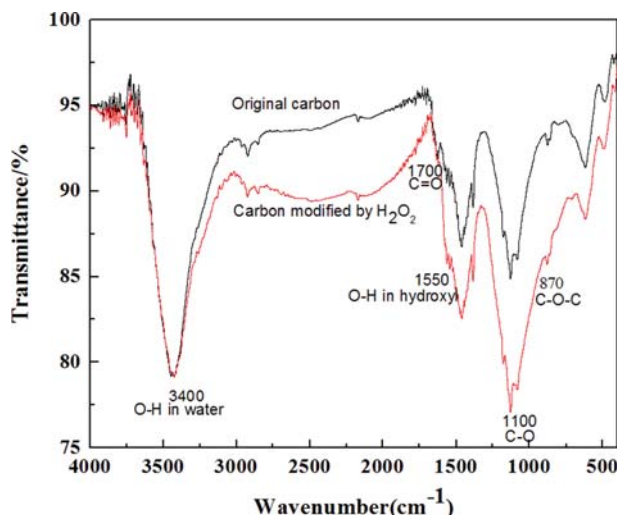


Fig. 4. FT-IR spectra of the original carbon and the carbon modified by H_2O_2 (3.75%).

with acidic groups.

Fig. 4 shows the FT-IR spectra of the original carbon and the carbon modified by H_2O_2 (3.75%). The spectral range around $3,400\text{ cm}^{-1}$ represents the hydroxyl and chemisorbed water O-H stretching vibration. The band at $1,700\text{ cm}^{-1}$ can be assigned to the C=O stretching vibration from carbonyl. The spectral range of about $1,550\text{ cm}^{-1}$ represents the carboxyl carbonate or surface hydroxyl

deformation vibration. The band centered around $1,100\text{ cm}^{-1}$ is ascribed to the C-O stretching vibration of hydroxyl [22-26]. The peak at 870 cm^{-1} resulted from C-O-C symmetric and asymmetric stretching vibration in the ether. It can be seen from Fig. 4 that there is no introduction of new groups on the carbon surface and the amount of carbonyl groups and hydroxyl groups increase after H_2O_2 modification.

The ESCALAB-250XI multifunctional photoelectron spectrometer was used to conduct a full spectrum analysis of the original carbon and the carbon modified by H_2O_2 at 1-1,200 eV, the C1s narrow spectrum was scanned within 278-297 eV and O1s narrow spectrum was obtained by scanning within 523-542 eV. The change of the surface groups on the carbon samples can be acquired through the fitting analysis of C1s and O1s.

As shown in Fig. 5, the peak in C1s can be resolved into six separate peaks: (1) Graphite carbons, (2) Carbon in phenols, alcohols and ethers; (3) Carbon in carbonyls and quinones; (4) Carbon in ester groups and anhydrides; (5) Carbon in carboxyl groups, and (6) $\pi\text{-}\pi^*$ shake-up. Table 2 lists the result of the peak fitting calculation. It can be seen from Table 2 that the proportion of the carbon in the form of graphite on the carbon surface decreases from 56.64% to 44.72% after the H_2O_2 modification. The percentage of the carbon in alcohol, aldehyde and ether increases from 8.50% to 21.05%. The content of the carbon in carbonyl and quinone slightly rises from 19.64% to 21.35% but the carbon in ester and anhydride decreases from 6.71% to 2.45%. The carbon in carboxyl is raised from 1.80% to 6.82%.

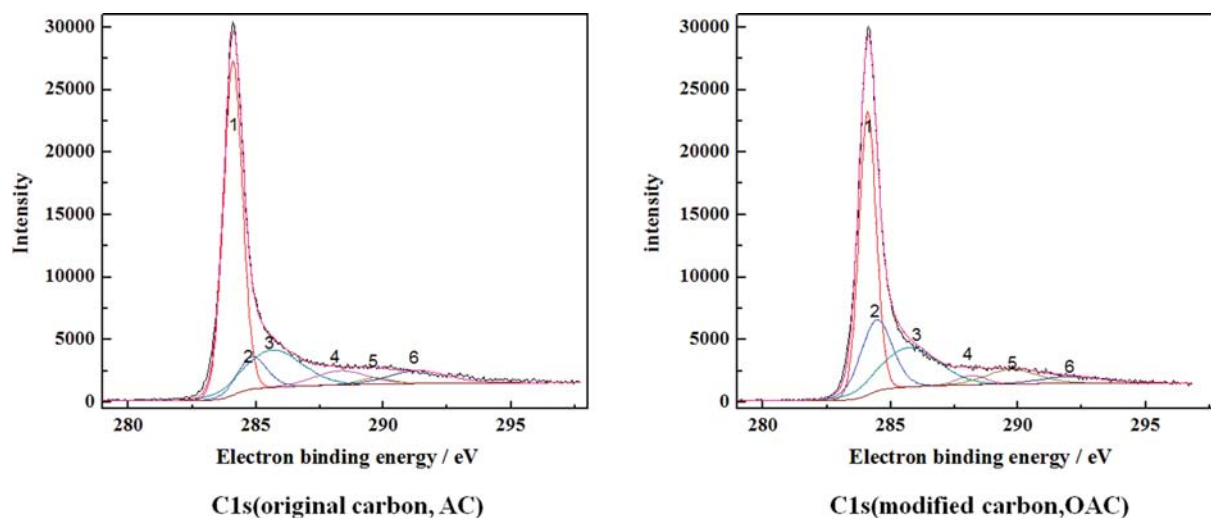


Fig. 5. C1s fitting curve of the original carbon and the carbon modified by H_2O_2 (3.75%).

Table 2. Fitted C1s peak parameters deduced from XPS for carbon samples

Peak	B.E (eV)	Assignment	AC (%)	OAC (%)
1	284.1	Graphite (C=C)	56.64	44.72
2	284.8	Aldehyde, alcohol and ether group (C-OH, C-O-C, C-O-R)	8.50	21.02
3	285.8	Carbonyl and quinone group (C=O)	19.64	21.35
4	288.3	Anhydride and ester group COOC-	6.71	2.45
5	289.4	Carboxyl COOH	1.80	6.82
6	291.5	$\pi\text{-}\pi^*$	6.70	3.64

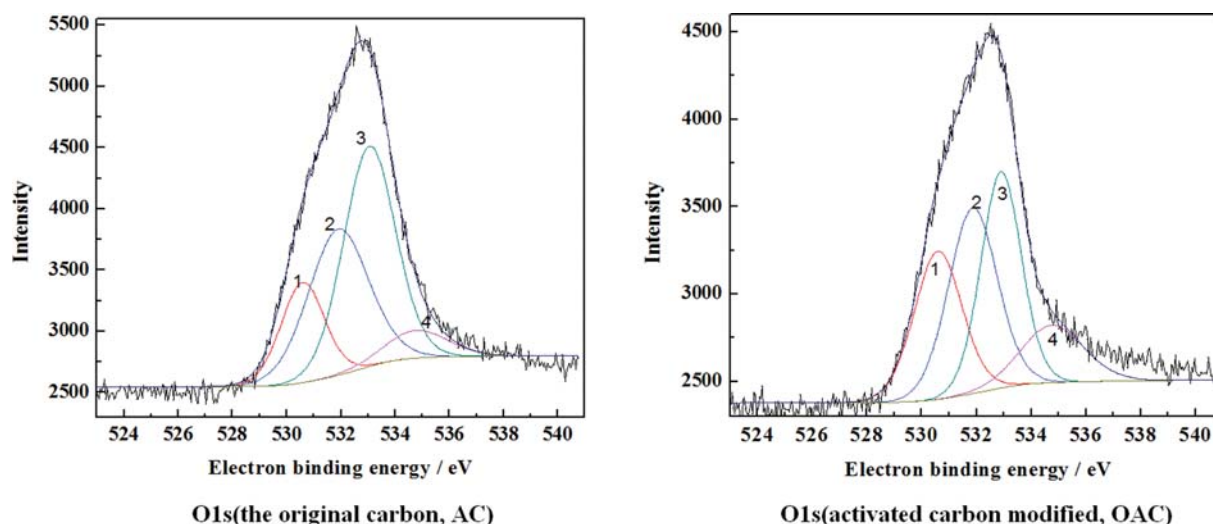


Fig. 6. O1s fitting curve of the original carbon and activated carbon modified by H₂O₂.

Table 3. Fitted O1s peak parameters deduced from XPS for carbon samples

Peaks	B.E (eV)	Assignment	AC (%)	OAC (%)
1	530.6	Carbonyl and quinone group (C=O)	16.63	24.94
2	531.9	C=O in mide, anhydride, ester group and oxygen in alcohol, ether group (C-OH, C-O-C)	33.52	31.78
3	533.2	C-O in anhydride and ester group (CO-O-R)	43.30	30.62
4	534.7	Carboxyl (COOR)	6.55	12.65

Table 4. Boehm titration results of carbon samples (H₂O₂ concentration)

H ₂ O ₂ concentration	Acidic groups (10 ⁻⁴ mol g ⁻¹)	Lactone (10 ⁻⁵ mol g ⁻¹)	Phenolic hydroxyl (10 ⁻⁵ mol g ⁻¹)	Carboxyl (10 ⁻⁵ mol g ⁻¹)	Basic groups (10 ⁻⁴ mol g ⁻¹)
0	0.667	1.62	4.53	0.519	8.69
1.50%	1.32	2.07	4.89	6.25	6.81
3.75%	1.54	2.41	5.76	7.22	6.62
4.50%	1.46	2.25	5.02	7.37	5.66

The O1s spectrum depicted in Fig. 6 is divided into four separate peaks: (1) Oxygen in carbonyl and quinone groups; (2) C=O in ester groups, amides, anhydrides, oxygen in ethers and alcohols; (3) C-O in the anhydride and esters; and (4) Oxygen in the carboxyl [27]. The peak resolution data listed in Table 3 shows that the proportion of the oxygen in the carbonyl group and the quinone group increases from 16.63% to 24.94%, and that of the oxygen in the carboxyl group increases from 6.55% to 12.65%. The percentage of the oxygen in the ester, anhydride, alcohol, ether decreases from 43.30% to 30.62%. And the oxygen in carboxyl rises from 6.55% to 12.65%. The XPS characterization suggests that the H₂O₂ treatment leads to great alteration in the surface chemistry on the carbon. The amount of carbonyl, carboxyl and hydroxyl groups increased conspicuously.

The Boehm titration data listed in Table 4 shows that the H₂O₂ modification results in an obvious increase in the total acidic groups, lactone, carboxyl and phenolic hydroxyl on the carbon surface. The amount of total acidic groups of the carbon sample impregnated in 3.75% H₂O₂ solution is 1.54×10⁻⁴ mol g⁻¹ while that of the orig-

inal carbon is only 6.67×10⁻⁵ mol g⁻¹. The carboxyl on this modified sample is 12-times that on the original carbon. The lactone on this sample is 2.41×10⁻⁵ mol g⁻¹ while that on the original carbon is 1.62×10⁻⁵ mol g⁻¹. The phenolic hydroxyl group increases from 4.53×10⁻⁵ mol g⁻¹ to 5.76×10⁻⁵ mol g⁻¹ after being treated with 3.75% H₂O₂ solution. It can also be noticed that the total basic groups on the modified samples are reduced obviously. For instance, the basic groups on the original carbon are 8.69×10⁻⁴ mol g⁻¹ while those on the sample treated with 3.75% H₂O₂ solution are 6.62×10⁻⁴ mol g⁻¹.

Table 4 also shows that the acidic groups on the carbon samples increase with the H₂O₂ concentration rising from 1.50% to 4.50% because higher H₂O₂ concentration accelerates the oxidation of the activated carbon and benefits the production of the oxygen-containing groups on the carbon surface. The rate of H₂O₂ decomposition to HOO· is 1,000 times that of the HOO⁻ generation rate, and the number of HOO· in the H₂O₂ solution increases with the H₂O₂ concentration. As a consequence, the carboxyl content increases as H₂O₂ concentration rises. Table 4 suggests that the phenolic hydroxyl of the samples modified with different H₂O₂ con-

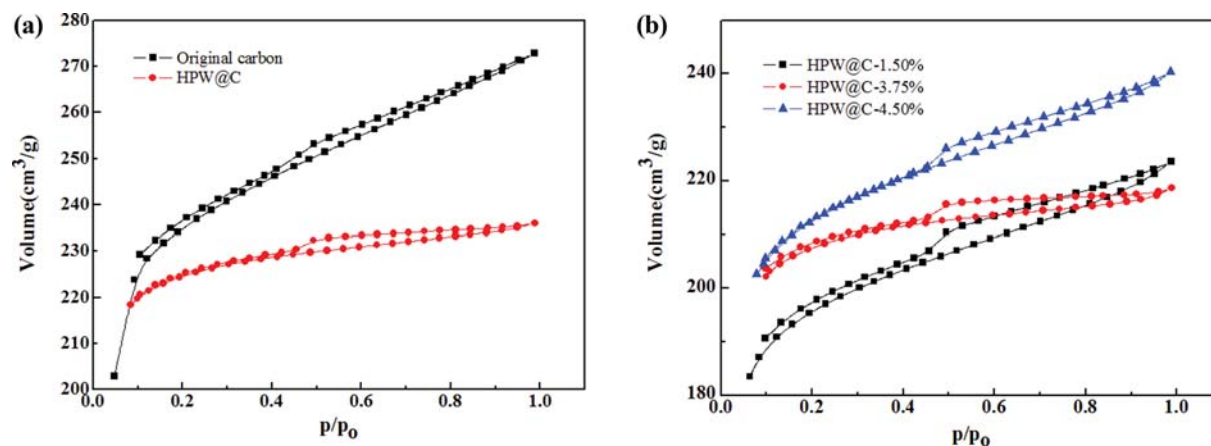


Fig. 7. N_2 adsorption-desorption isotherms (H_2O_2 concentration).

centration is in the order of $3.75\% > 4.50\% > 1.50\%$. The reason may be that high H_2O_2 concentration helps the oxidation of C-H to C-OH. But more phenolic hydroxyl groups will be oxidized to carbonyl groups if the H_2O_2 concentration increases further.

Fig. 7 is the N_2 adsorption-desorption isotherms of different samples. Fig. 7(a) demonstrates that the adsorption capacity of HPW@C decreases obviously compared with that of the original activated carbon because of the HPW adsorption on the carbon surface. Fig. 7 also proves that the modification with H_2O_2 solution enhances the adsorption ability of the HPW@C catalyst. The adsorption abilities of the HPW@C catalysts prepared with the carbon impregnated in H_2O_2 solution are in the sequence of $4.50\% > 3.75\% \approx 1.50\%$. Greater adsorption ability is favorable for the catalytic activity of the catalysts.

Table 5 lists the physical characteristics of original activated carbon and HPW@C catalysts. It can be seen from Table 5 that the specific surface area and pore volume of activated carbon loaded with HPW are clearly reduced because the HPW molecules covering carbon pores thicken the walls of the holes, reduce the pore size and block the holes [24–26]. The total surface of the original activated carbon is $757.2 \text{ m}^2 \text{ g}^{-1}$ while that of HPW@C is $690.8 \text{ m}^2 \text{ g}^{-1}$. The total pore volume of HPW@C was reduced to $0.3651 \text{ cm}^3 \text{ g}^{-1}$ from $0.4221 \text{ cm}^3 \text{ g}^{-1}$ of the original activated carbon.

Table 5 also shows that the specific surface of the catalyst increases with H_2O_2 concentration. But the micropore surface of the catalyst prepared with the carbon oxidized by H_2O_2 is in the order of $3.75\% > 4.50\% > 1.50\%$. The surface area of mesopores increases from $17.9 \text{ m}^2 \text{ g}^{-1}$ to $55.2 \text{ m}^2 \text{ g}^{-1}$ when H_2O_2 concentration increases from 3.75% to 4.50%. The reason may be that some pores are pro-

duced due to the oxidation of the activated carbon by H_2O_2 . But some micropores may be turned into mesopores as H_2O_2 concentration increases from 3.75% to 4.50% because of the reaction between the micropore and H_2O_2 .

Though the HPW@C catalyst prepared with the original carbon has greater surface area than the catalyst prepared with the carbon modified by H_2O_2 , the catalytic activity of the former is inferior to that of the latter because the latter holds more acidic groups than the former. Hence, it can be concluded that acidic groups play a more important role than the surface area in the catalytic oxidation of MX to IPA. The increase of acidic groups on the carbon surface is favorable for the adsorption of MX, especially the polar compounds 3-IMA, M-TA and 3-CBA on HPW@C catalyst, which accelerates the production of IPA from the oxidation of MX. The carbon treated with 3.75% H_2O_2 holds more acidic groups than the carbon treated with 4.50% H_2O_2 so that the catalytic capacity of the HPW@C catalyst prepared with the former is superior to that of the HPW@C catalyst prepared with the latter despite the fact that the former has smaller surface area than the latter. The catalytic capacity of the HPW@C catalyst prepared with the carbon modified with 1.50% H_2O_2 exhibits the worst catalytic activity among these three catalysts prepared with the modified carbon because it has the fewest acidic groups and the smallest surface area.

2. Effect of Impregnation Temperature

The temperature of the carbon sample impregnated in H_2O_2 solution may affect the oxidation of activated carbon by H_2O_2 . Five carbon samples were impregnated in 3.75% H_2O_2 solution for 8 h at 30°C , 40°C , 45°C , 50°C and 55°C , respectively, followed by being carbonized at 700°C for 4 h. The $H_3PW_{12}O_{40}$ @C catalysts

Table 5. Physical characteristics of the samples (H_2O_2 concentration)

Impregnation concentration	S_{BET} ($\text{m}^2 \text{ g}^{-1}$)	S_{mic} ($\text{m}^2 \text{ g}^{-1}$)	S_{BJH-A} ($\text{m}^2 \text{ g}^{-1}$)	V_{total} ($\text{cm}^3 \text{ g}^{-1}$)	V_{mic} ($\text{cm}^3 \text{ g}^{-1}$)	D_{BJH} (nm)
Original carbon	757.2	674.3	82.9	0.4221	0.3337	2.23
HPW@C	690.8	670.4	20.4	0.3651	0.3423	2.11
HPW@C-1.50%	622.3	567.2	55.2	0.3459	0.2836	2.22
HPW@C-3.75%	633.7	615.8	17.9	0.3382	0.3173	2.14
HPW@C-4.50%	668.0	612.7	55.2	0.3718	0.3102	2.23

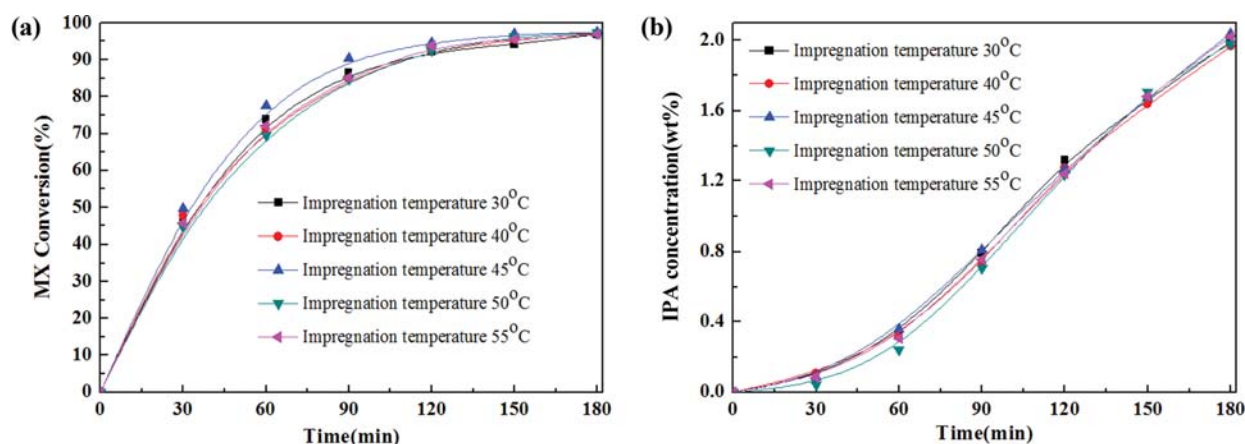


Fig. 8. Effect of H₂O₂ impregnation temperature on MX oxidation. 215 °C, 3.0 MPa, air fluent: 1.0 L min⁻¹, stirring speed: 300 r/min, HPW@C: 16.0 g L⁻¹, MX: 3.53% (wt), Co²⁺: 0.069% (wt), H₂O: 4.0% (wt), HAC: 400 ml.

prepared with the carbon samples obtained were applied to accelerate the oxidation of MX to IPA. Fig. 8 shows the changes of MX conversion and IPA concentration with reaction time.

Fig. 8(a) shows that the MX oxidation rates of the samples impregnated at different temperature differ little. After 180 min operation, the MX conversions obtained by the HPW@C catalysts prepared with the carbon samples impregnated at 30 °C, 40 °C, 45 °C, 50 °C and 55 °C are 96.87%, 97.20%, 97.35%, 97.30% and 96.90%.

Fig. 8(b) shows that the IPA yields obtained by the HPW@C catalysts prepared with the carbon samples impregnated at different temperature are similar. After 180 min reaction, the IPA engendered by the catalysts prepared with the samples immersed at 30 °C, 40 °C, 45 °C, 50 °C and 55 °C are 1.99% (wt), 1.97% (wt), 2.04% (wt), 1.98% (wt) and 2.02% (wt), respectively. The difference of the catalytic activities of the catalysts prepared is little when the impregnation temperature ranges from 30 °C to 55 °C.

The Boehm data shown in Table 6 suggest that the carboxyl groups increase with the impregnation temperature because a higher oxidation temperature may be favorable for the formation of the carboxyl groups. Lactones also increase with the impregnation temperature because more carboxyl groups is of benefit to the production of lactone from the reaction between carboxyl groups and

phenolic hydroxyl groups. But the phenolic hydroxyl groups decrease with the impregnation temperature because the oxidation rate of phenolic hydroxyl to carbonyl is significantly accelerated at higher impregnation temperatures [22].

The physical characteristics depicted in Table 7 show that S_{BET} increases as the impregnation temperature rises from 30 °C to 40 °C because more micropores are produced due to the more violent oxidation reaction between the carbon and H₂O₂ as the impregnation temperature rises. But S_{BET} decreases with the impregnation temperature rising over 40 °C because micropores are destroyed due to the fierce oxidation of carbon by H₂O₂ at higher reaction temperature. The mesopores reduce with the impregnation temperature because more mesopores are damaged if the impregnation temperature goes up. Fig. 8 demonstrates that the sequence of the adsorption capacity of HPW@C is in concert with that of their S_{BET} .

Though the HPW@C catalyst prepared with the carbon impregnated at 45 °C holds the smallest S_{BET} and S_{mic} among these three samples, its catalytic activity is similar to those of the other catalysts because it holds the most acidic groups on its surface area. S_{BET} of the HPW@C catalyst prepared with the carbon impregnated at 40 °C is bigger than that of the catalyst prepared with the carbon

Table 6. Boehm titration results of carbon samples (impregnation temperature)

Impregnation temperature	Acidic groups (10 ⁻⁴ mol g ⁻¹)	Lactone (10 ⁻⁵ mol g ⁻¹)	Phenolic hydroxyl (10 ⁻⁵ mol g ⁻¹)	Carboxyl (10 ⁻⁵ mol g ⁻¹)	Basic groups (10 ⁻⁴ mol g ⁻¹)
30 °C	1.44	1.10	9.52	3.82	6.97
40 °C	1.31	2.39	5.97	4.74	6.12
45 °C	1.54	2.41	5.76	7.22	6.62

Table 7. Physical structure of HPW@C catalysts (impregnation temperature)

Impregnation temperature	S_{BET} (m ² g ⁻¹)	S_{mic} (m ² g ⁻¹)	S_{BJH-A} (m ² g ⁻¹)	V_{total} (m ³ g ⁻¹)	V_{mic} (m ³ g ⁻¹)	D_{BJH} (nm)
30 °C	676.4	621.9	54.5	0.3685	0.3287	2.15
40 °C	737.9	690.9	46.9	0.3999	0.3457	2.17
45 °C	633.7	615.8	17.9	0.3382	0.3173	2.14

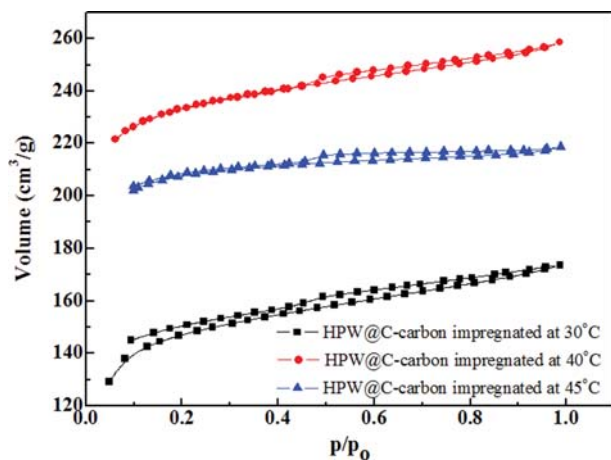


Fig. 9. N_2 adsorption-desorption isotherms (impregnation temperature).

impregnated at 30 °C, they have the same catalytic performance because of the latter having more acidic groups.

3. Effect of Impregnation Time

The time of the carbon impregnated in H_2O_2 solution may influence the oxidation of carbon by H_2O_2 . Four carbon samples were impregnated in 3.75% H_2O_2 solution for 6 h, 7 h, 8 h and 9 h, respectively, followed being calcined at 700 °C for 4 h. The $H_3PW_{12}O_{40}@C$ catalysts prepared with the carbon samples obtained were used to catalyze the oxidation of MX to IPA. The experimental results in Fig. 10 show that 7 h is the optimal impregnation time.

Fig. 10(a) shows that the highest MX oxidation rate is obtained by the HPW@C catalyst prepared with the carbon impregnated

for 7 h. After 180 min operation, the MX conversion acquired by the sample impregnated for 7 h is 99.02% while those obtained by the samples impregnated for 6 h, 8 h and 9 h are 97.23%, 97.70% and 96.87%, respectively. In Fig. 10(b) the IPA produced by the HPW@C catalyst prepared with the carbon impregnated for 7 h is higher than any other catalysts. After 180 min reaction, the IPA concentration obtained by the sample impregnated for 7 h is 2.09% (wt), while those obtained by the samples impregnated for 6 h, 8 h and 9 h are 1.84% (wt), 1.97% (wt) and 1.97% (wt), respectively.

The Boehm data in Table 8 show that carboxyl group increases with impregnation time because the prolongation of the oxidation time is favorable for the production of carboxyl groups. The lactones also increase with the impregnation time because more lactones are formed due to more carboxyls combining with phenolic hydroxyls. The phenolic hydroxyl groups increase as the impregnation time extends from 6 h to 7 h due to more carbon oxidized to phenolic hydroxyl groups by H_2O_2 . However, the phenolic hydroxyl groups are reduced with the impregnation time prolonging to 8 h because more phenolic hydroxyls are consumed in the production of lactones. The sample impregnated in H_2O_2 solution for 8 h holds the most acidic groups.

Fig. 11 shows that the adsorption capacities of the HPW@C catalysts decrease with the impregnation time, which is similar to the order of their S_{BET} . The physical characteristics listed in Table 9 show that the mesopores decrease with the impregnation time because more mesopores are destroyed due to the long reaction time between carbon and H_2O_2 . S_{mic} of the HPW@C catalyst prepared with the carbon impregnated for 7 h is the biggest among those of these three samples. Some micropores are produced from the carbon oxidation by H_2O_2 as the impregnation time increases from

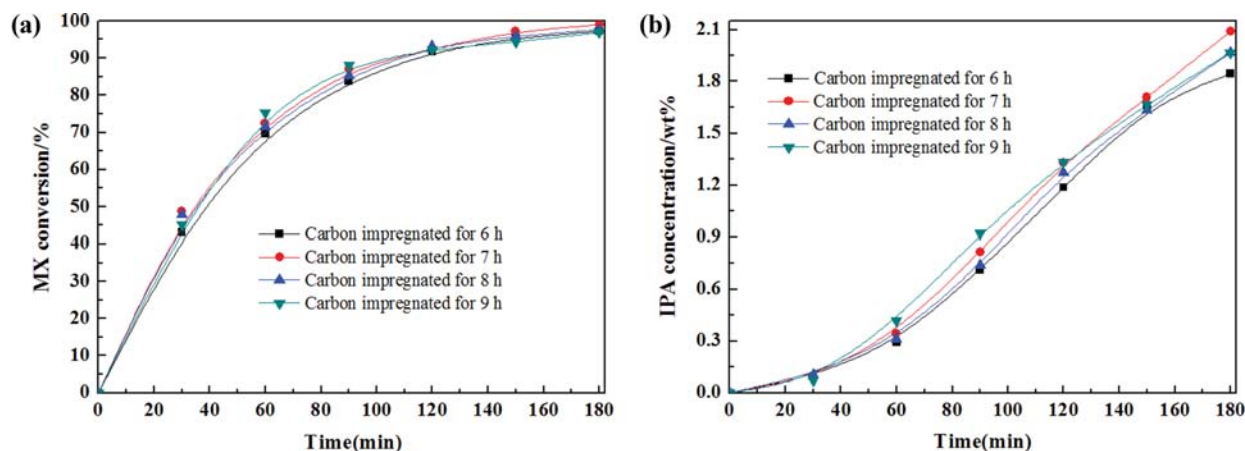


Fig. 10. Effect of H_2O_2 impregnation time on MX oxidation. 215 °C, 3.0 MPa, air fluent: 1.0 L min^{-1} , stirring speed: 300 r/min, HPW@C: 16.0 $g\ l^{-1}$, MX: 3.53% (wt), Co^{2+} : 0.069% (wt), H_2O : 4.0% (wt), HAC: 400 ml.

Table 8. Boehm titration results of carbon samples (impregnation time)

Impregnation time	Acidic groups ($10^{-4}\ mol\ g^{-1}$)	Lactone ($10^{-5}\ mol\ g^{-1}$)	Phenolic hydroxyl ($10^{-5}\ mol\ g^{-1}$)	Carboxyl ($10^{-5}\ mol\ g^{-1}$)	Basic groups ($10^{-4}\ mol\ g^{-1}$)
6 h	1.16	1.79	5.93	3.86	6.62
7 h	1.41	2.26	7.52	4.27	6.31
8 h	1.31	2.39	5.97	4.74	6.12

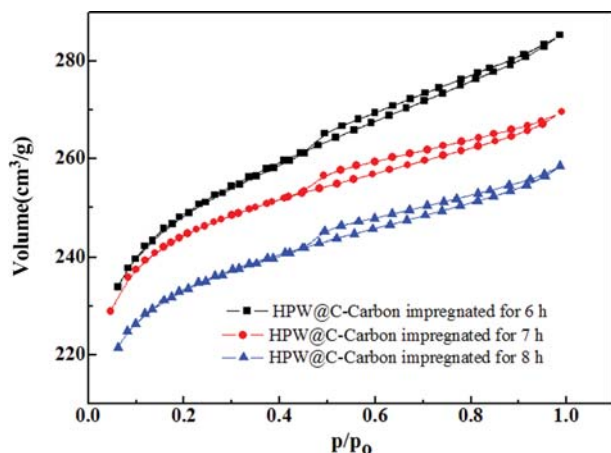


Fig. 11. N₂ adsorption-desorption isotherms (impregnation time).

6 h to 7 h. But more micropores are destroyed when the impregnation time prolongs from 7 h to 8 h due to the long time erosion caused by H₂O₂.

The HPW@C catalyst prepared with the carbon impregnated for 7 h exhibits the best catalytic activity because it has the most acidic groups. Though S_{BET} of the HPW@C catalyst prepared with

the carbon impregnated for 6 h is bigger than that of the HPW@C catalyst prepared with the carbon impregnated for 8 h, the latter shows better catalytic activity than the former because the latter holds more acidic groups.

4. Effect of Calcination Temperature

Calcination is an important step in the modification of carbon with H₂O₂. To test the effect of calcination temperature, three carbon samples were calcined for 4 h at 600 °C, 700 °C and 800 °C, respectively, after being impregnated in 3.75% H₂O₂ solution for 7 h at 40 °C. The MX oxidation results catalyzed by the HPW@C catalysts prepared with the carbon samples obtained shown in Fig. 12 illustrate that 700 °C is the best calcination temperature.

It can be seen from Fig. 12 that the HPW@C catalyst prepared with the carbon sample carbonized at 700 °C gets the highest MX oxidation rate and IPA yield. After 180 min reaction, the MX conversion obtained by the sample calcined at 700 °C is 99.02% while those obtained by the samples calcined at 600 °C and 800 °C are 96.95% and 97.56%, respectively. The IPA produced by the samples calcined at 600 °C, 700 °C and 800 °C are 1.90% (wt), 2.09% (wt), and 1.96% (wt), respectively.

The Boehm data shown in Table 10 show that the carboxyl groups decrease with the calcination temperature. The reason may be that some groups on the surface of the activated carbon may decom-

Table 9. Physical structure of HPW@C catalysts (impregnation time)

Impregnation time	S_{BET} (m ² g ⁻¹)	S_{mic} (m ² g ⁻¹)	S_{BJH-A} (m ² g ⁻¹)	V_{total} (cm ³ g ⁻¹)	V_{mic} (cm ³ g ⁻¹)	D_{BJH} (nm)
6 h	790.1	713.0	77.0	0.4413	0.3576	2.23
7 h	780.7	732.6	48.1	0.4171	0.3622	2.14
8 h	737.9	690.9	46.9	0.3999	0.3457	2.17

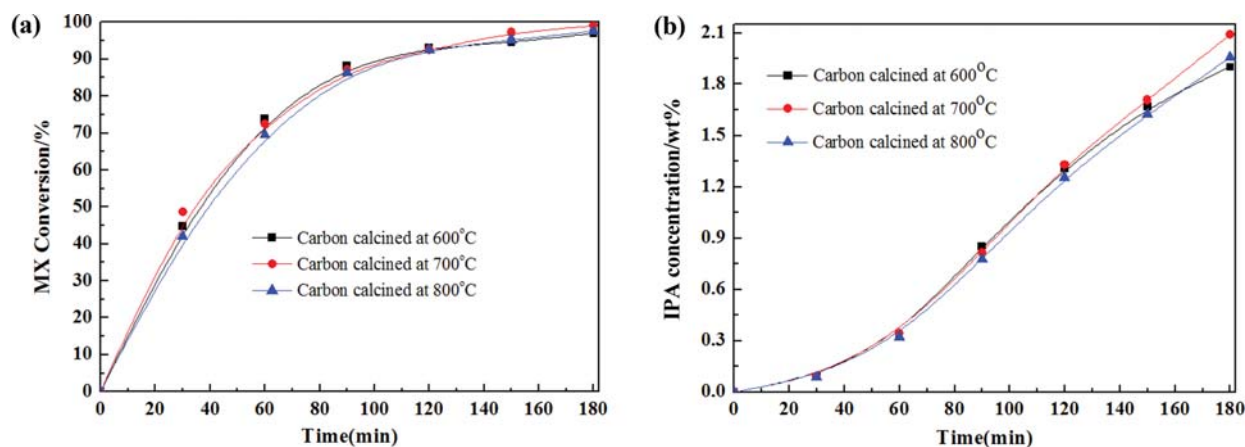


Fig. 12. Effect of calcination temperature on reaction in H₂O₂ modification. 215 °C, 3.0 MPa, air fluent: 1.0 L min⁻¹, string speed: 300 r/min, HPW@C: 16.0 g l⁻¹, MX: 3.53% (wt), Co²⁺: 0.069% (wt), H₂O: 4.0% (wt), HAC: 400 ml.

Table 10. Boehm titration results of carbon samples (calcination temperature)

Calcination temperature	Acidic groups (10 ⁻⁴ mol g ⁻¹)	Lactone (10 ⁻⁵ mol g ⁻¹)	Phenolic hydroxyl (10 ⁻⁵ mol g ⁻¹)	Carboxyl (10 ⁻⁵ mol g ⁻¹)	Basic groups (10 ⁻⁴ mol g ⁻¹)
600 °C	1.29	1.88	5.21	5.20	6.71
700 °C	1.41	2.26	7.52	4.27	6.31
800 °C	1.25	3.60	5.10	3.81	6.14

Table 11. Physical structure of HPW@C catalysts (calcination temperature)

Calcination temperature	S_{BET} ($m^2 g^{-1}$)	S_{mic} ($m^2 g^{-1}$)	S_{BJH-A} ($m^2 g^{-1}$)	V_{total} ($cm^3 g^{-1}$)	V_{mic} ($cm^3 g^{-1}$)	D_{BJH} (nm)
600 °C	785.0	705.8	79.1	0.4365	0.3501	2.22
700 °C	780.7	732.6	48.1	0.4171	0.3622	2.14
800 °C	795.4	736.2	59.3	0.4395	0.3710	2.21

pose at high temperature in N_2 atmosphere [31-33]. The lactone increases with the carbonization temperature due to more lactones produced at higher temperature.

The physical characteristics depicted in Table 11 show that S_{mic} increases with the calcination temperature because more micropores are produced due to more acidic groups decomposing at higher temperature. S_{BJH-A} decreases from $79.1 m^2 g^{-1}$ to $48.1 m^2 g^{-1}$ as the carbonization temperature rises from 600 °C to 700 °C, but increases again to $59.3 m^2 g^{-1}$ when the carbonization temperature goes up further to 800 °C. S_{BET} changes little as the carbonization temperature ranges from 600 °C to 800 °C. Fig. 13 shows that the adsorption capacities of the HPW@C catalysts are in accordance with their

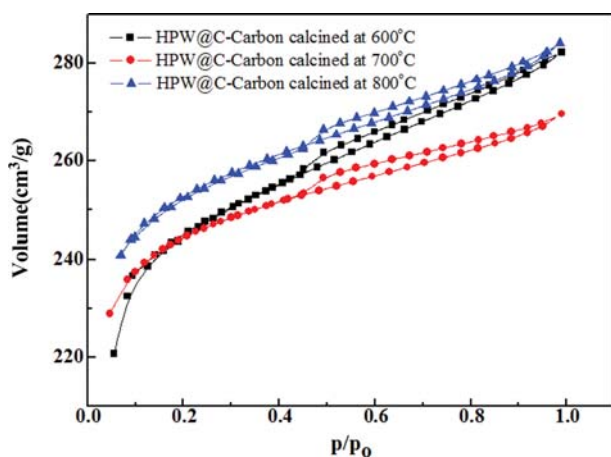
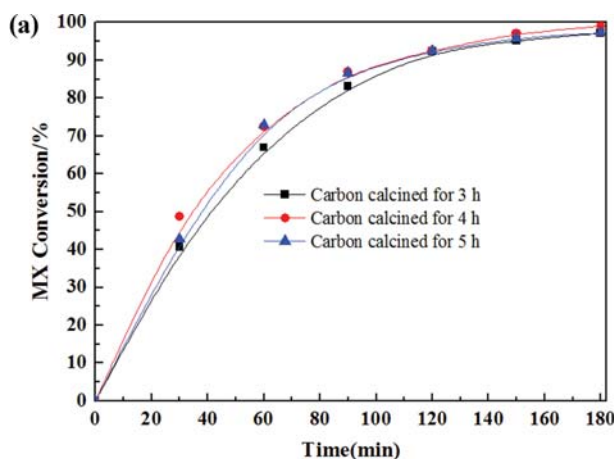


Fig. 13. N_2 adsorption-desorption isotherms (calcination temperature).



S_{BET} .

The HPW@C catalyst prepared with the carbon calcined at 700 °C displays the best catalytic activity because it has the most acidic groups among these three samples. Though the HPW@C catalyst prepared with the carbon calcined at 800 °C holds greater S_{BET} than the HPW@C catalyst prepared with the carbon calcined at 600 °C, these two samples exhibit similar catalytic ability due to the latter owning more acidic groups.

5. Effect of Calcination Time

Three carbon samples were calcined at 700 °C for 3 h, 4 h and 5 h, respectively, after being impregnated in 3.75% H_2O_2 solution for 7 h at 40 °C. The HPW@C catalysts prepared with the carbon samples acquired were applied to speed up the oxidation of MX to IPA.

The MX oxidation results depicted in Fig. 14 prove that 4 h is the best carbonization time. The MX conversion after 180 min operation obtained by the samples calcined for 3 h, 4 h and 5 h was 96.95%, 99.02% and 97.56%, respectively. The IPA produced by the sample calcined for 3 h, 4 h and 5 h is 1.96% (wt), 2.09% (wt) and 1.90% (wt), respectively.

The Boehm data listed in Table 12 reflect that phenolic hydroxyl groups and carboxyl groups decrease as the calcination time increases from 3 h to 4 h. The reason is that more phenolic hydroxyl groups and carboxyl groups are consumed and decomposed with the elongation of the carbonization time. The lactones increase as the activation time extends from 3 h to 5 h because more lactones are produced due to the reaction between phenolic hydroxyl groups and carboxyl groups with a long reaction time.

Fig. 15 shows that the adsorption capacity of the HPW@C catalysts decreases with the calcination time. The physical characteris-

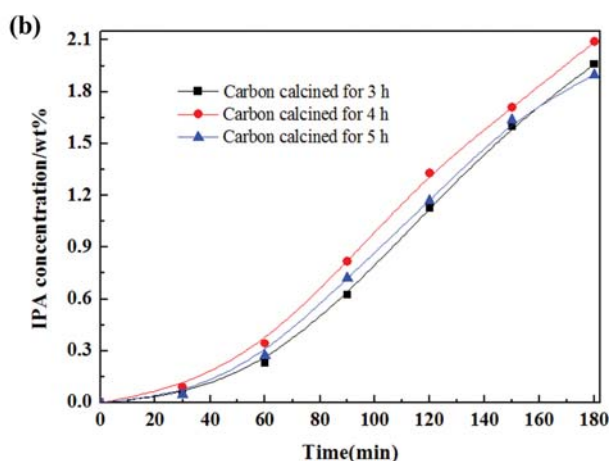


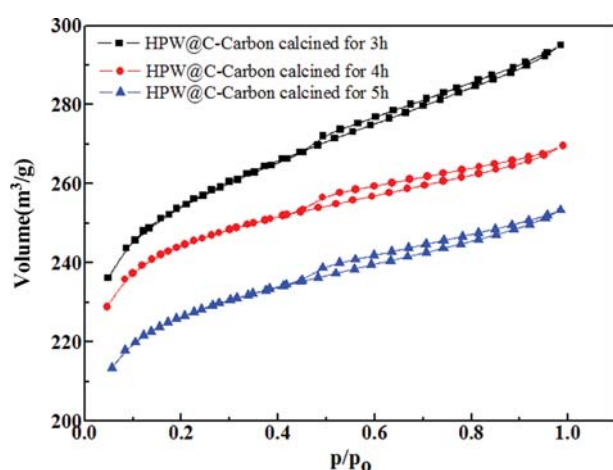
Fig. 14. Effect of calcination time on reaction in H_2O_2 modification. 215 °C, 3.0 MPa, air fluent: $1.0 L min^{-1}$, stirring speed: 300 r/min, HPW@C: $16.0 g l^{-1}$, MX: 3.53% (wt), Co^{2+} : 0.069% (wt), H_2O : 4.0% (wt), HAC: 400 ml.

Table 12. Boehm titration results of carbon samples (calcination time)

Calcination time	Acidic groups (10 ⁻⁴ mol g ⁻¹)	Lactone (10 ⁻⁵ mol g ⁻¹)	Phenolic hydroxyl (10 ⁻⁵ mol g ⁻¹)	Carboxyl (10 ⁻⁵ mol g ⁻¹)	Basic groups (10 ⁻⁴ mol g ⁻¹)
AC-3 h	1.32	1.01	7.73	4.47	6.38
AC-4 h	1.41	2.26	7.52	4.27	6.31
AC-5 h	1.40	3.25	6.99	3.80	6.83

Table 13. Physical structure of HPW@C catalysts (calcination time)

Calcination time	S _{BET} (m ² g ⁻¹)	S _{mic} (m ² g ⁻¹)	S _{BJH-A} (m ² g ⁻¹)	V _{total} (cm ³ g ⁻¹)	V _{mic} (cm ³ g ⁻¹)	D _{BJH} (nm)
3 h	816.8	731.7	85.1	0.4565	0.3633	2.24
4 h	780.7	732.6	48.1	0.4171	0.3622	2.14
5 h	719.0	665.9	53.2	0.3919	0.3317	2.18

**Fig. 15. N₂ adsorption-desorption isotherms.**

tics shown in Table 13 reveal that S_{BET} and S_{mic} decrease obviously with the calcination time prolonging from 3 h to 5 h because more micropores are destroyed with a longer calcination time at high temperature.

Though the HPW@C catalyst prepared with the carbon calcined for 4 h has smaller S_{BET} than the catalyst prepared with the carbon calcined for 3 h, the former shows more excellent catalytic activity than the latter because the former has more acidic groups. Though the HPW@C catalyst prepared with the carbon calcined for 3 h has bigger S_{BET} than the catalyst prepared with the carbon calcined for 5 h, these two samples exhibit similar catalytic performance because the latter has more acidic groups.

CONCLUSIONS

A study was made to improve the catalytic activity of HPW@C catalyst by oxidizing the carbon with H₂O₂ solution. Some conclusions drawn from the experiments are as follows:

(1) The catalytic capability of HPW@C catalyst in the production of IPA from MX was ameliorated after the activated carbon treated with H₂O₂ solution.

(2) The best modification condition was calcining the carbon at

700 °C for 4 h after being impregnated in 3.75% H₂O₂ solution at 40 °C for 7 h.

(3) The surface characterization reveals that the H₂O₂ modification gave rise to an increase in the acidic groups and a reduction in the basic groups on the carbon surface. The increase of acidity is beneficial to the catalytic activity of the HPW@C catalyst in the oxidation of MX to IPA. The catalytic ability of the HPW@C catalyst relies on its surface chemical characteristics and physical property. The surface chemistry plays a more important role than the physical property.

(4) The MX conversion after 180 min reaction acquired by the HPW@C catalysts prepared from the activated carbon modified in the best condition was 3.81% over that obtained by the HPW@C catalyst prepared from the original carbon. The IPA produced by the former is 46.2% over that produced by the latter.

ACKNOWLEDGEMENTS

The present work is supported by the NSFC (No. 21176081).

REFERENCES

1. A. K. Suresh, M. M. Sharma and T. Sridhar, *Ind. Eng. Chem. Res.*, **39**, 3958 (2008).
2. C. X. Xu, K. D. Yang, Z. L. Liu, Z. Z. Qin, W. He, Q. W. Dai, J. J. Zhang and F. Zhang, *Chinese J. Chem. Eng.*, **22**, 305 (2014).
3. H. F. Lv, S. Q. Wu, N. Liu, X. L. Long and W. K. Yuan, *Chem. Eng. J.*, **172**, 1045 (2011).
4. X. L. Long, Z. H. Wang, S. Q. Wu, S. M. Wu, H. F. Lv and W. K. Yuan, *J. Ind. Eng. Chem.*, **20**, 100 (2014).
5. X. L. Hao, X. W. Zhang and L. C. Lei, *Carbon*, **47**, 153 (2009).
6. E. Vega, J. Lemus, A. Anfruns, R. Gonzalez-Olmos, J. Palomar and M. J. Martin, *J. Hazard. Mater.*, **258-259**, 77 (2013).
7. W. Liu, J. Zhang, C. Cheng, G. Tian and C. Zhang, *Chem. Eng. J.*, **175**, 24 (2011).
8. K. Kuśmierk, A. Świątkowski, K. Skrzypczyńska, S. Błażewicz and J. Hryniewicz, *Korean J. Chem. Eng.*, **34**, 1081 (2017).
9. Q. Q. Guo, W. Jing, S. Z. Cheng, Z. G. Huang, D. K. Sun, Y. Q. Hou and X. J. Han, *Korean J. Chem. Eng.*, **32**, 2257 (2015).
10. H. Park, D. H. Yeom, J. Kim and J. K. Lee, *Korean J. Chem. Eng.*,

- 32, 178 (2015).
11. Q. Liu, M. Ke, P. Yu, F. Liu, H. Q. Hu and C. C. Li, *Korean J. Chem. Eng.*, **35**, 137 (2018).
 12. Z. H. Wang, Z. L. Yang, S. M. Wu and X. L. Long, *Int. J. Chem. Reactor Eng.*, **13**, 413 (2015).
 13. C. Chen, X. Li, Z. Tong, Y. Li and M. Li, *Appl. Surf. Sci.*, **315**, 203 (2014).
 14. Y. Xue, B. Gao, Y. Yao, M. Inyang, M. Zhang, A. R. Zimmerman and K. S. Ro, *Chem. Eng. J.*, **200-202**, 673 (2012).
 15. X. L. Song, H. Y. Liu, L. Cheng and Y. X. Qu, *Desalination*, **255**, 78 (2010).
 16. H. P. Boehm, *Carbon*, **32**, 759 (1994).
 17. S. Biniak, G. Szymański, J. Siedlewski and A. Świątkowski, *Carbon*, **35**, 1799 (1997).
 18. R. M. Ladera, M. Ojeda, J. L. G. Fierro and S. Rojas, *Catal. Sci. Technol.*, **5**, 484 (2014).
 19. W. Alharbi, E. F. Kozhevnikova and I. V. Kozhevnikov, *Acs Catal.*, **5**, 7186 (2015).
 20. D. B. Vončina and A. Majcen-Le-Marechal, *Dyes Pigm.*, **59**, 173 (2003).
 21. M. Domingo-García, F. J. López Garzón and M. J. Pérez-Mendoza, *J. Colloid Interface Sci.*, **248**, 116 (2002).
 22. X. Song, H. Liu, C. Lei and Y. Qu, *Desalination*, **255**, 78 (2010).
 23. C. Moreno-Castilla, M. V. López-Ramón and F. Carrasco-Marín, *Carbon*, **38**, 1995 (2000).
 24. C. Moreno-Castilla, F. Carrasco-Marín, F. J. Maldonado-Hódar and J. Rivera-Utrilla, *Carbon*, **36**, 145 (1998).
 25. P. Vinke, M. van der Eijk, M. Verbree, A. F. Voskamp and H. van Bekkum, *Carbon*, **32**, 675 (1994).
 26. V. Gómez-Serrano, M. Acedo-Ramos, A. J. López-Peinado and C. Valenzuela-Calahorra, *Fuel*, **73**, 387 (1994).
 27. U. Zielke, K. J. Hüttinger and W. P. Hoffman, *Carbon*, **34**, 983 (1996).
 28. Z. Liu, S. Cao, S. Wang, W. Zeng, T. Zhang, P. Li and F. Lei, *J. Chem. Eng. Japan*, **48**, 29 (2015).
 29. R. G. Prado, M. L. Bianchi, E. G. D. Mota, S. S. Brum, J. H. Lopes and M. J. D. Silva, *Waste & Biomass Valorization*, **8**, 1 (2017).
 30. A. S. Badday, A. Z. Abdullah and K. T. Lee, *Renewable Energy*, **62**, 10 (2014).
 31. Y. Zhi and J. Liu, *Chemosphere*, **144**, 1224 (2016).
 32. J. J. Luo, J. Lu, Q. Niu, X. Chen, Z. Wang and J. Zhang, *Fuel*, **160**, 440 (2015).
 33. H. Guedidi, L. Reinert, Y. Soneda, N. Bellakhal and L. Duclaux, *Arabian J. Chem.*, **304**, S3584 (2014).